

190

# Advances in Powder Metallurgy & Particulate Materials - 1997

Proceedings of the 1997 International Conference on  
Powder Metallurgy & Particulate Materials sponsored by  
the Metal Powder Industries Federation and APMI  
International, June 29 - July 2, Chicago, Illinois.

Compiled by

**Robert A. McKotch**  
President - Press Division  
Gasbarre Products, Inc.

and

**Richard Webb**  
Vice President - Operations  
Norwalk Powdered Metals Company

**METAL POWDER INDUSTRIES FEDERATION  
APMI INTERNATIONAL**

105 College Road East, Princeton, New Jersey 08540-6692  
TEL (609) 452-7700 FAX (609) 987-8523



# OPTIMIZATION OF THE COMBUSTION SYNTHESIS/QUASI-ISOSTATIC PRESSING PROCESSING SEQUENCE IN TIC-BASED CERMETS

E. Olevsky, E. Kristofetz, C. Uzoigwe and M. Meyers

*NSF Institute for Mechanics and Materials  
University of California, San Diego  
9500 Gilman Dr., La Jolla CA 92093-0404, USA*

## ABSTRACT

A combination of combustion synthesis and quasi-isostatic pressing (QIP) is used for production of high-density titanium carbide / Ti-Ni cermets. The goals of the study include minimization of final porosity and the control of the microstructure and phase composition. Parameters which are considered for the optimization include the initial sample porosity, the chemical composition, the time delay between ignition and consolidation.

## 1. INTRODUCTION

Self-Propagating High Temperature Synthesis (SHS) which utilizes exothermic, sustaining reactions between the constituents has assumed significance for production of intermetallic, ceramic and cermet materials. Being a very rapid processing technique, SHS tremendously increases productivity in comparison with conventional techniques. However, because of the thermal-explosive character of SHS, an excessive porosity is usually formed in the products. This generates a need for subsequent densification which is often troublesome for highly deformation-resistant materials such as titanium carbides.

A simultaneous process combining combustion synthesis (SHS) and densification would be appropriate for the solution of this technological problem. Combustion synthesis followed by quasi-isostatic pressing in a granular medium (QIP) is an example of such a process [1-5]. Powder pressure transmitting medium (PTM) provides lateral confinement and redistributes the applied axial load. Herewith, there are the process optimization parameters which enable the production of highly-dense material under the SHS - QIP processing sequence. For the treatment of Ti-C-Ni powder systems where Ti-Ni is used in the capacity of a toughness-increasing binder, these parameters are:

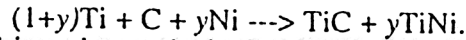
- initial porosity;
- concentration of the intermetallic matrix phase;
- the time delay between ignition and the beginning of consolidation;
- parameters of the microstructure of the green body (particle, grain and pore sizes and morphology);

- pressure applied under QIP;
- time of QIP.

The present work includes computational analysis of the influences of the first three parameters on the final properties of the Ti-C-Ni specimen produced by the SHS - QIP processing sequence.

## 2. EXPERIMENTAL PROCEDURE

The following basic reaction was studied:



Powder combinations were mixed in order to obtain final product compositions corresponding to varying volume fractions of TiNi from 0.3 to 0.5. The powders were loaded under argon into polyethylene jars and dry mixed with burundum™ grinding media (4:1 by weight) for 48 hours. Then the powders were baked in a vacuum oven for a minimum of 48 hours at approximately 100°C and a pressure less than 100 mm Hg to remove adsorbed water. After baking, the powders were uniaxially pressed into 25 g green compacts with a diameter of 32.6 mm and height of approximately 10 mm.

The experimental configuration for the synthesis/densification process is shown in Figure 1. The fixture used to contain the samples during the processing was a thick walled steel cylinder filled with an alumina based granular medium from Superior Graphite. The granular medium redistributed the applied axial load to create stress profiles more similar to those obtained during isostatic pressing. It also acted as a thermal insulator to reduce heat losses to the steel die and punch during the reaction and to allow temperatures to approach the adiabatic condition.

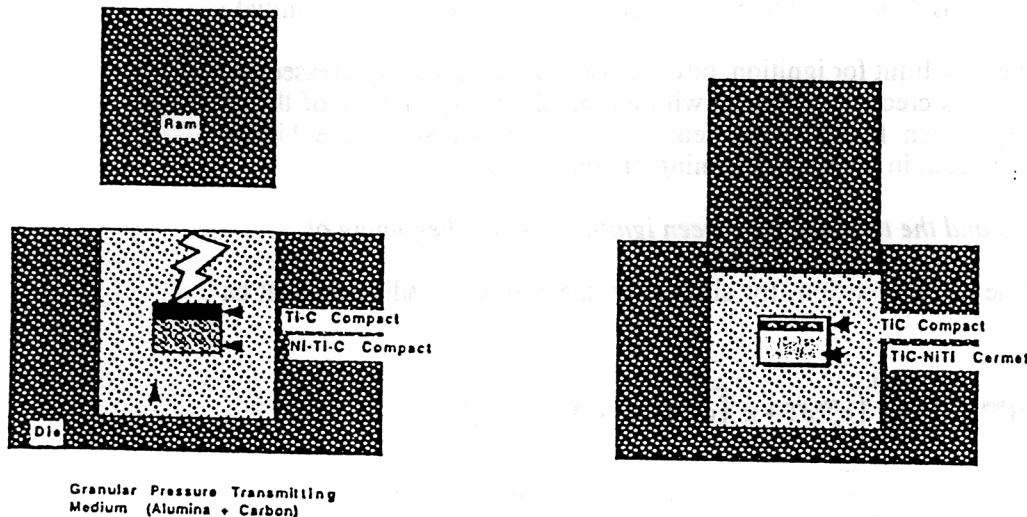


Fig. 1 Experimental configuration for the synthesis/densification

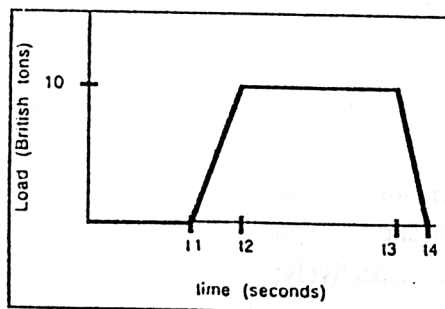


Fig.2 A schematic representation of the loading as a function of time

Figure 2 shows a schematic representation of the loading as a function of time. The time  $t_1$  represents the time between ignition and the beginning of consolidation. Since sample reaction results in the expulsion of impurity gases, ignition is marked by the ejection of granular media from the die. In the present study,  $t_1$  was between 3 and 18 sec. The difference between  $t_2$  and  $t_1$  ( $t_2 - t_1$ ) is the time to maximum load. On the Enerpac H-frame 100 ton capacity hydraulic press used in these experiments, the time to reach a load of 10 British tons was approximately 5 seconds. The quantity ( $t_3 - t_2$ ) is the

holding time under QIP and was set at 15 seconds. The unloading time ( $t_4 - t_3$ ) was about second.

### 3. ANALYSIS OF THE INFLUENCE OF THE OPTIMIZATION PARAMETERS ON THE FINAL PRODUCT DENSITY

#### *3.1. Initial porosity*

The experiments indicate that the main influence of the initial porosity is on sample integrity and ignition. Samples with a green density less than 60% were extremely fragile and tend to break during handling. Evidently with such high porosity, there is insufficient mechanical interlocking between particles to keep the specimen intact.

For samples with green densities between approximately 60-75% combustion was successfully initiated. The samples were loaded to 10 British tons after a time  $t_2$  (Fig. 2), of 15 seconds. The average final porosity was determined using a computer software program by Media Cybernetics entitled "Image Pro-Plus." Once an image was acquired by the computer, the threshold level for material phases was set manually to match the observed contrast between regions. The average porosity was calculated from 10 different images acquired along the longitudinal cross-section of the sample. The final porosity was determined to be between 1-2%, irrespective of the initial density.

To determine an upper density limit for ignition, powder was cold isostatically pressed in at 180 MPa for 30 seconds. This created a compact with an initial density of 83% of theoretical. All attempts to ignite this specimen failed. Apparently, for small porosities, the higher conductivity stops the reaction front in the very beginning of combustion.

#### *3.2. Concentration of TiC and the time delay between ignition and the beginning of consolidation*

Due to the very short time of combustion, for simplicity, the following adiabatic heat balance conditions can be assumed:

$$\begin{cases} \kappa \cdot H^{TiC} + (1 - \kappa)H^{TiNi} = (1 - \kappa) \int_{T_0}^{T_{comb}} c_p^{TiNi} dT + \kappa \int_{T_0}^{T_{comb}} c_p^{TiC} dT, T_0 < T_{comb} < T_m^{TiNi} \\ \kappa \cdot H^{TiC} + (1 - \kappa)H^{TiNi} = (1 - \kappa) \left[ \int_{T_0}^{T_{comb}} c_p^{TiNi} dT + \lambda_{TiNi} \cdot H_m^{TiNi} \right] + \kappa \int_{T_0}^{T_{comb}} c_p^{TiC} dT, T_{comb} = T_m^{TiNi} \\ \kappa \cdot H^{TiC} + (1 - \kappa)H^{TiNi} = (1 - \kappa) \left[ \int_{T_0}^{T_{comb}} c_p^{TiNi} dT + H_m^{TiNi} \right] + \kappa \int_{T_0}^{T_{comb}} c_p^{TiC} dT, T_m^{TiNi} < T_{comb} < T_m^{TiC} \\ \kappa \cdot H^{TiC} + (1 - \kappa)H^{TiNi} = (1 - \kappa) \left[ \int_{T_0}^{T_{comb}} c_p^{TiNi} dT + H_m^{TiNi} \right] + \kappa \left[ \int_{T_0}^{T_{comb}} c_p^{TiC} dT + \lambda_{TiC} \cdot H_m^{TiC} \right], T_{comb} = T_m^{TiC} \end{cases}$$

where  $\kappa$  is the mass concentration of TiC;  $H^{TiC}$  and  $H^{TiNi}$  are latent heats of formation of TiC and TiNi phases, respectively;  $H_m^{TiNi}$  and  $H_m^{TiC}$  are the latent heat of melting of TiNi and TiC phases, respectively;  $\lambda_{TiNi}$  and  $\lambda_{TiC}$  are the mass concentrations of liquid TiNi and TiC, respectively; and  $c_p^{TiNi}$  and  $c_p^{TiC}$  are heat capacities of TiC and TiNi phases, respectively;  $T_0$  is the room temperature (298K);  $T_{comb}$  is the maximum temperature of the combustion;  $T_m^{TiNi}$  is the melting temperature of the TiNi phase.

In Eqs. (1) it is assumed that TiNi is the only intermetallic phase formed under combustion.

Table 1. Material Properties [6]

$H^{TiC}$ (kJ/mol)	184.5
$H^{TiNi}$ (kJ/mol)	64.4
$H_m^{TiNi}$ (kJ/mol)	32.5
$H_m^{TiC}$ (KJ/mol)	71.1
$c_p^{TiC}$ solid ( $JK^{-1}mol^{-1}$ )	$50+0.85 \cdot 10^{-3}T-14.87 \cdot 10^{-5}T^2+1.94 \cdot 10^{-6}T^3$
$c_p^{TiC}$ liquid ( $JK^{-1}mol^{-1}$ )	62.76
$c_p^{TiNi}$ solid ( $JK^{-1}mol^{-1}$ )	$53+9.623 \cdot 10^{-3}T-0.812 \cdot 10^{-6}T^2$
$c_p^{TiNi}$ liquid ( $JK^{-1}mol^{-1}$ )	67.92
$T_m^{TiNi}$ (Kelvin)	1583
$T_m^{TiC}$ (Kelvin)	3290

Using the values for materials properties represented in Table 1, one can obtain from Eqs. 1 the relationship between the combustion temperature and the mole concentration of TiC (Fig. 3). The relationship between the mole concentration of melted TiNi (when combustion temperature is equal to the melting point of TiNi) and the mole concentration of TiC is shown in Fig. 4.

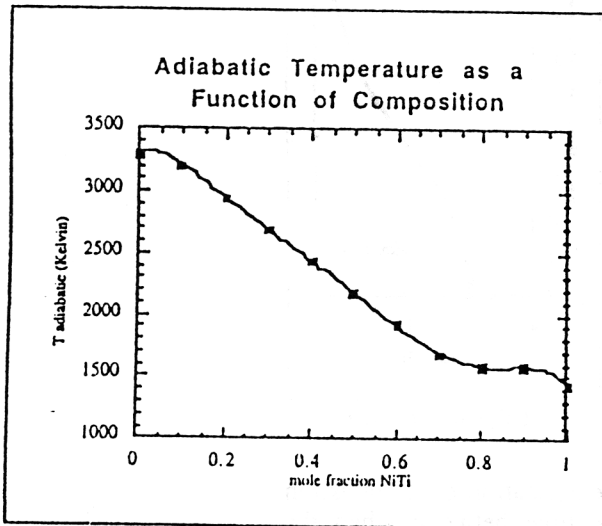


Fig. 3 Final reaction temperature as a function of composition

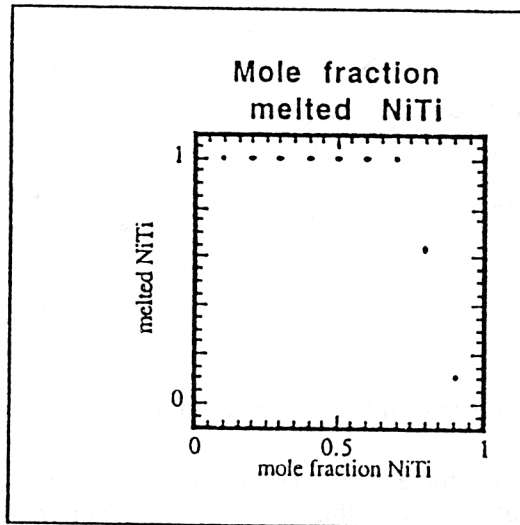


Fig 4. Fraction of melted NiTi as a function of composition

### 3.3. Influence of cooling and the time delay between ignition and the beginning of consolidation

Here, attention is turned to nonisothermal effects of cooling. This analysis is based upon the idea of an infinitely-extended pressure-transmitting medium.

In this analysis, it is assumed that the thermal conductivity of the porous body is sufficiently larger than that of the pressure-transmitting medium (i.e. PTM) so that its temperature distribution is approximately uniform. With this assumption, the rate-of-change of temperature for the porous body is given by:

$$\frac{dT}{dt} = -\left(\frac{h}{\rho C_p}\right)\left(\frac{S}{V}\right)(T - T_\infty) \quad (2)$$

where  $T$ ,  $\rho$ ,  $C_p$ ,  $S$ , and  $V$  are the temperature, density, heat capacity, surface area, and volume of the porous body, respectively;  $h$  and  $T_\infty$  are the heat-transfer coefficient and temperature of the PTM; and  $t$  is time. Note that in assuming Eq. (2) to be valid, it is implicitly assumed that the thermal conductivity of the PTM is sufficiently large such that the thermal gradients within it are small. For the cylindrical body geometry, the surface area/volume ratio is given by:

$$\frac{S}{V} = \frac{2}{H}\left(1 + \frac{H}{R}\right) \quad (3)$$

where  $H$  and  $R$  are the height and radius of the cylinder, respectively. Due to the infinity of space occupied by the PTM,  $T_\infty = 293\text{K}$  (room temperature). Equation (2) corresponds to the solution of the problem of cooling for the range of temperatures. The results of the solution of Eq. (2) for different mol concentrations of the TiC phase are represented in Fig. 5.

Here we use the following idea (proved experimentally - see below): for reaching a high final density, the temperature of the specimen in the beginning of QIP should be equal to the melting point of the TiNi binder. Here the following values of geometry and material parameters were used:  $H=10\text{mm}$ ,  $R=16.3\text{ mm}$ ,  $h=50\text{ W/(mK)}$ . Density and heat capacity  $C_p$  were calculated as the weight average of TiC and TiNi densities and heat capacities (see Table 1), respectively, for corresponding weight concentrations of the constituents.

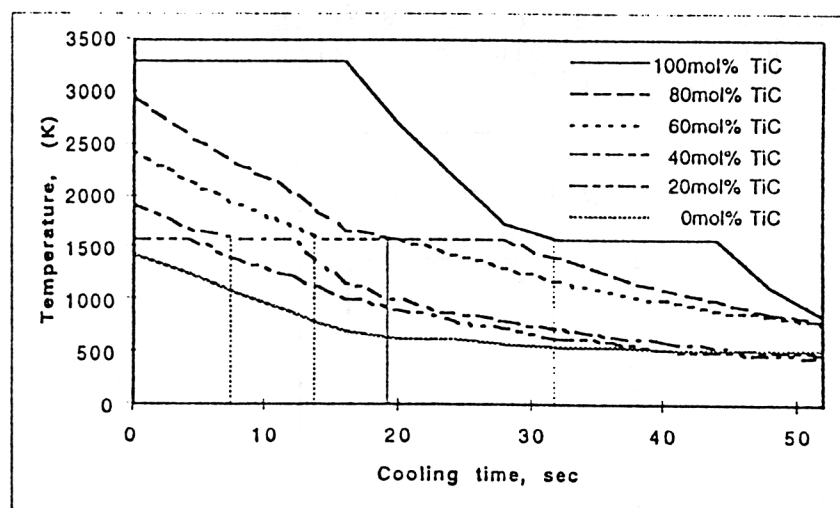


Fig. 5 Temperature evolution during time delay between combustion and densification

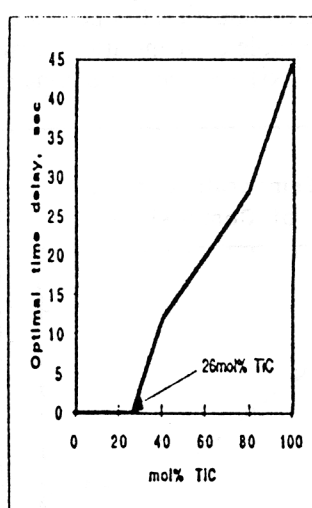


Fig. 6 Optimal time delay

It is important to note that there is a time window for successful densification of combustion synthesized materials. For pure TiC this window corresponds to the time between when the reaction is completed and when the temperature of the sample falls below the ductile to brittle transition temperature. Densification studies by Merzhanov [7] determined that for TiC the temperature of the compact drops below its transition temperature approximately 5 to 10 seconds after ignition.

Adding Ni to the reaction, systematically lowers the calculated adiabatic temperature and shortens the time at which the sample is above the ductile to brittle transition temperature. This detrimental loss of temperature is offset, however, by the melting of the Ni. Studies by LaSalvia [8] revealed that the presence of liquid nickel (melting point  $1453^\circ\text{C}$ ), extends the window for successful densification to between 10 to 15 seconds after ignition. In the present work on combustion synthesized TiC-TiNi cermets the available time for successful densification was extended even further, because liquid TiNi surrounds the solid TiC spherical particles until  $1310^\circ\text{C}$  and aids consolidation.

From Fig. 5 one obtains (see Fig. 6) the optimal dependence between the mole concentration of TiC and the time delay.

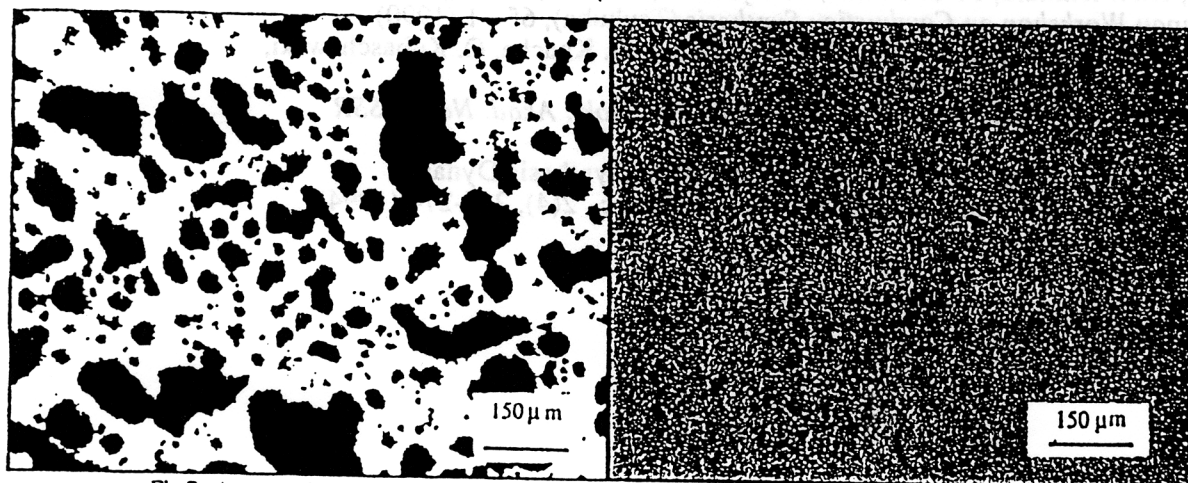


Fig.7a As reacted material

Fig.7b Reacted material loaded to 10 British tons after a delay time of 15 seconds

For a 30 vol% TiNi-TiC cermet (0.76 mole fraction TiC) the predicted upper time limit for successful densification is approximately 25 seconds. Figure 7 compares the microstructure of the as reacted material (Fig.7a) to the same material loaded to 10 British tons after a delay time of 15 seconds (Fig.7b). The final porosity is less than 1.5%.

### CONCLUSIONS

1. For initiation of ignition of Ti-Ni-C powder system, 25% - 40% initial porosity range is chosen as an optimal one.
2. For reaching a high final density, the temperature of the specimen in the beginning of QIP should be equal to the melting point of the TiNi binder.
3. Optimal dependence between the mol concentration of TiC and the time delay is determined using the heat balance and heat transfer equations.

### ACKNOWLEDGMENT

The research is supported by the Institute for Mechanics and Materials under the National Science Foundation Grant No. MSS 92-18300 and by the U.S. Army Research Office under its MURI program (Contract NO. DAAH 04-96-1-0376).

### REFERENCES

- [1]. R.V. Raman, S.V. Rele, S. Poland, J. LaSalvia, M.A. Meyers, and A.R. Niiler, The one-step synthesis of titanium-carbide tiles, *J. Metals*, N3, 23-25 (1995)
- [2]. J.C. LaSalvia, D.K. Kim, and M.A. Meyers, Effect of Mo on microstructure and mechanical properties of TiC-Ni-based cermets produced by combustion synthesis - impact forging technique, *Mat. Sci. Eng.*, A206, 71-80 (1996)
- [3]. R.V. Raman, M.A. Janney, S.A. Sastri, An innovative processing approach to fabricate fully-dense near-net-shape advanced material parts, *World Congress on Powder Metallurgy*, Washington DC, 131 (1996)
- [4]. Z.Y. Fu, W.M. Wang, R.Z. Yuan, Z.A. Munir, Fabrication of cermets by SHS-QP method, *Int. J. SHS*, 2, 307-313 (1993)

- [5]. P.H. Shingu, K.N. Ishihara, F. Ghonome, T. Hyakawa, M. Abe, K. Tagushi, *Proc. of the 1st US-Japan Workshop on Combustion Synthesis* (Tsukuba), 65-71 (1990)
- [6]. Thermomechanical Properties of Inorganic Substances, I, O. Knacke, O. Kubaschewski, K. Hesselman (eds.), Springer-Verlag (1991)
- [7]. A.G. Merzhanov, V.I. Yukhvid, and I.P. Borovinskaya, *Dokl. Akad. Nauk SSSR* 255(1), 503-506 (1980).
- [8] J.C. LaSalvia, M.A. Meyers, and D.K. Kim, Combustion Synthesis/Dynamic  
Densification of TiC-Ni Cermets, *J. of Mats. Syn. and Proc.*, 2(4), 255-274 (1994).



190

# Advances in Powder Metallurgy & Particulate Materials - 1997

Proceedings of the 1997 International Conference on  
Powder Metallurgy & Particulate Materials sponsored by  
the Metal Powder Industries Federation and APMI  
International, June 29 - July 2, Chicago, Illinois.

Compiled by

**Robert A. McKotch**  
President - Press Division  
Gasbarre Products, Inc.

and

**Richard Webb**  
Vice President - Operations  
Norwalk Powdered Metals Company

**METAL POWDER INDUSTRIES FEDERATION  
APMI INTERNATIONAL**

105 College Road East, Princeton, New Jersey 08540-6692  
TEL (609) 452-7700 FAX (609) 987-8523

